Computational Fluid Dynamics Simulation of Impeller and Seal Rotordynamics

A Technical Report submitted to the Department of Mechanical Engineering

Presented to the Faculty of the School of Engineering and Applied Science
University of Virginia • Charlottesville, Virginia

In Partial Fulfillment of the Requirements for the Degree
Bachelor of Science, School of Engineering

Pascale Starosta

Spring, 2021

On my honor as a University Student, I have neither given nor received unauthorized aid on this assignment as defined by the Honor Guidelines for Thesis-Related Assignments

Signature  Date 5/11/2021
Pascale Starosta

Approved _____ Date _____
Cori Watson-Kassa, Research Scientist, ROMAC Lab UVA

Computational Fluid Dynamics Simulation of Impeller and Seal Rotordynamics

CFD VALIDATION OF NON-AXISYMMETRIC FLOW AND ROTORDYNAMIC FORCES IN A SHROUDED CENTRIFUGAL COMPRESSOR

Introduction

Interactions between a centrifugal impeller and a working fluid can generate forces that act on the rotor in various directions. Predicting fluid-induced forces such as these is essential in the design of turbomachinery [Guinzburg et al., 1994]. These forces are called rotordynamic forces, and can be broken down into the directions they act in: the normal force in the direction of the eccentricity and the tangential force which is normal to the eccentricity. Direct stiffness, damping, and mass (K_{xx}, C_{xx}, M_{xx}) and cross-coupled stiffness, damping, and mass (K_{xy}, C_{xy}, M_{xy}) coefficients are used to express rotordynamic forces. The effective damping coefficient, composed of the cross-coupled stiffness and direct damping coefficients and the whirling frequency, is used to determine the rotordynamic instability of operating machinery [Song et al., 2019].

Centrifugal compressors are used in a variety of turbomachinery. The reduction of rotordynamic instability is necessary to prevent mechanical failures and maximize performance of machinery [Song et al., 2019]. Song et al. used an experimental test rig to examine the effect of non-axisymmetric flow on the impeller, shroud, and labyrinth seal of a centrifugal compressor. However, computational studies examining the total effect of impeller blades, an eye-labyrinth seal, and shroud cavity have not been previously performed.

In previous studies, bulk-flow models were developed for the individual components of a centrifugal compressor, but these were never analyzed collectively as a group. A labyrinth seal model was developed by Iwatsubo [Iwatsubo, 1980], and a shroud rotordynamic force model was created by Childs [Childs]. Attempts have been made on these models to improve the prediction accuracy of each piece, but they were not modified to show the combined effects on a centrifugal compressor's performance.

Computational Fluid Dynamics (CFD) offers the benefit of reducing costs for testing impellers in this type of system, while investigating the full non-axisymmetric compressor flow field. Unlike an experimental setup, CFD doesn't require physical materials or parts. This requirement is what makes experimental setups less financially effective. Compared to bulk flow analysis, which has been previously used on individual components of a centrifugal compressor, CFD analysis does not rely on wall and interface constants that can change with the geometry [Kamouni, 2016]. While CFD is computationally expensive, the program can easily be altered to adjust the model and test a variety of parameters.

The fluid flow in the shroud cavity of a centrifugal compressor has been analyzed previously. The CFD calculations performed by Soldatova presented detailed information on the flow through a shroud cavity. This shroud cavity additionally had a labyrinth seal with 4 teeth, similar to the Song et al. full impeller model with a labyrinth seal with 3 teeth [Soldatova, 2017].

CFD has been used previously to determine the fluid forces acting on a shrouded, centrifugal compressor, face-seal impeller. Eccentricity on the face-seal impeller was also investigated in this paper [Kim, 2016]. Kamouni performed CFD analysis to simulate the driving forces and dynamic coefficients in an eccentric labyrinth seal. This type of seal is often used as a compressor eye seal, but this analysis also fails to simulate the entire system of seal, shroud, and

impeller [Kamouni, 2016]. Muttalli et al. used ANSYS CFX-14 to evaluate the head, power, efficiency, and cavitation of a centrifugal pump compressor. This analysis did not include a shroud or labyrinth seal around the impeller to catch any back flow [Muttalli et al., 2014].

All previous CFD analyses performed on centrifugal compressor impellers failed to analyze a full system composed of an impeller, shroud, and labyrinth seal. This study examines this system and the effect of non-axisymmetric flow through it. The results from the simulation are validated using the experimental results obtained by Song et al. on a physical model of the same centrifugal compressor system.

Because the model used by Song et al. had a smaller shroud gap than is considered normal for shrouded impellers, the shroud cavity simulated with CFD in Soldatova's paper was also generated and tested. Using both of these models simultaneously allowed the results to be verified as well as propagated to a similar model but with larger dimensions.

Procedure

1. Geometry

The first seal geometry modeled for this paper is the same geometry evaluated experimentally in Song et al. [Song et al., 2019]. A shrouded impeller with an eye-labyrinth seal is modeled. In the computational model, the tips of the seal teeth are flattened so that the mesh can generate on the ends of them. The geometric parameters used to create the model are given in the table below.

Table 1. Geometric Parameters for Song et al.

Parameter	Value
Impeller exit diameter (D)	153.24 mm
Blade exit length (d)	9.19 mm
Back-sweep angle	44.5 degrees
Number of blades	16
Number of seal teeth	3
Seal clearance (C)	0.55 mm
Seal height (h)	3 mm
Seal pitch (L)	7 mm
Rotor radius (R)	46.79 mm
Shroud cavity height at inlet (1)	1.38 mm
Shroud cavity height at middle (2)	2.5 mm
Shroud cavity height at exit (3)	3.55 mm

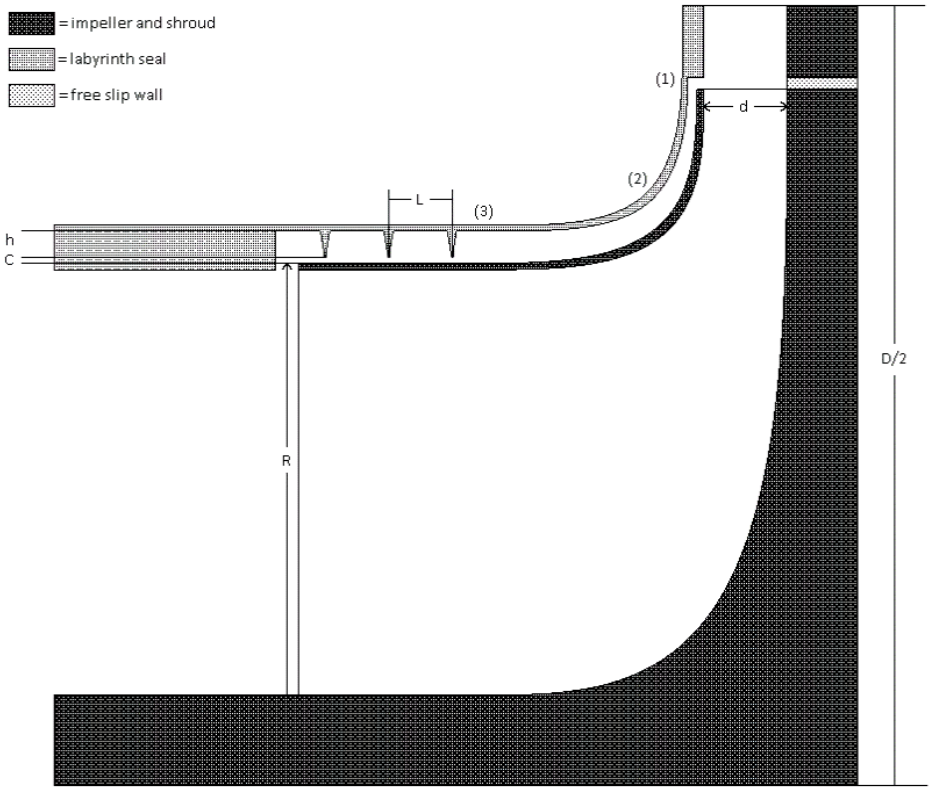

Figure 1: Cross section of the impeller, shroud, and labyrinth seal from the Song et al. model.

The pressure difference between the impeller exit and inlet results in leakage flow through the labyrinth seal. This leakage flow will travel from the diffuser inlet at the exit of the impeller through the seal back to the impeller inlet, and mix with the main flow entering the impeller.

The shroud cavity from Soldatova's paper was also modeled since it had a more normally sized shroud cavity width. The geometric parameters for this model are listed below in Table 2.

Table 2. Geometric Parameters for Soldatova

Parameter	Value
Impeller exit diameter (D_2)	409.85 mm
Number of seal teeth	4
Seal clearance (C_2)	0.50 mm
Rotor diameter (D_R)	204.95 mm
Shroud cavity height at inlet (b_2)	5.94 mm

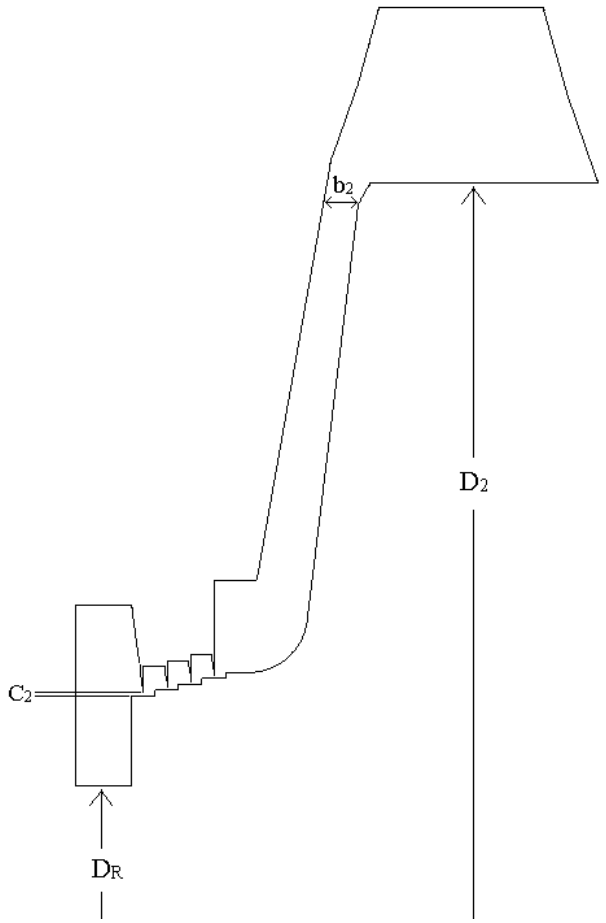

Figure 2: Cross section of the shroud cavity modeled from Soldatova's paper.

Only the shroud cavity was modeled in Soldatova's paper, unlike the full impeller, shroud, and seal system in Song et al.. Consequentially, only the shroud cavity was modeled for this paper, so the results could be validated against the results obtained by Soldatova for the same geometry with larger shroud width than the Song et al. model.

2. Numerical Methodology

The computational model was designed in ANSYS CFX using the above geometric parameters. The flattened teeth ends were 0.2 mm across. The mesh was generated using an element size the same size as the clearance of the seal (0.55 mm). The number of elements in the mesh was 8,803,483 and the mesh type was one with tetrahedral elements.

The rotating speed was set to 36,900 rpm. The inlet total pressure used was 100.5 kPa. The outlet static pressure was calculated using the equation given for the relationship between the two pressures in Song et al.:

$$\Psi = (P_o - P_i)/(\rho_i R\omega) \quad (1)$$

This yielded an outlet pressure of 140 kPa. [Song et al.].

An inverse model was created of the solid impeller, shroud, and seal system to simulate the domain of fluid flow in the impeller and between the shroud and the seal.

The boundary conditions for the 4 domains (inlet, outlet, rotating, and stationary) were set using the same values that had were used in the experiments by Song et al. [Song et al., 2019].

Table 3. Boundary conditions for Song et al.

Operating Condition	Value
Inlet Total Pressure	100.5 kPa
Outlet Average Static Pressure	140 kPa
Rotating Speed	36900 rpm

In order to simulate the rotation of the impeller inside the seal, the reference frame was set to be rotating at the given speed, and the inlet, outlet, and impeller all rotated with it. The exterior labyrinth seal was set as a counter rotating wall. This would prevent the mesh from deforming on the impeller blades, as would happen if this piece was chosen to rotate against the frame.

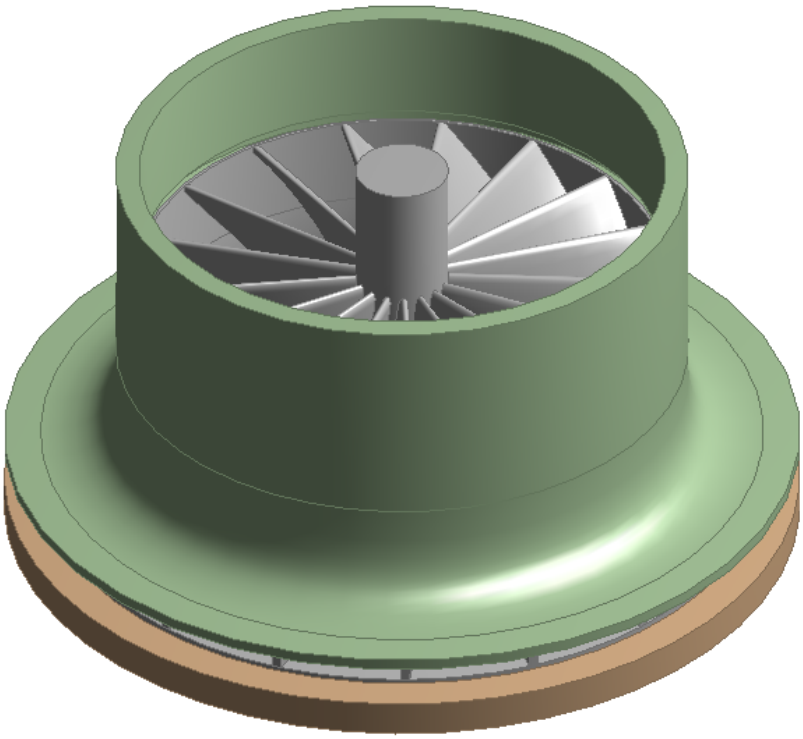

Figure 3: Model of the complete impeller, shroud, and seal system from Song et al.

The proximity function was chosen to generate the mesh in CFX. The k-ε turbulence model is used for the CFD analysis, and the walls are set as being adiabatic.

The free slip wall was set as a separate boundary condition to model that gap before the diffuser that existed in the experimental setup used by Song et al. [Song et al., 2019].

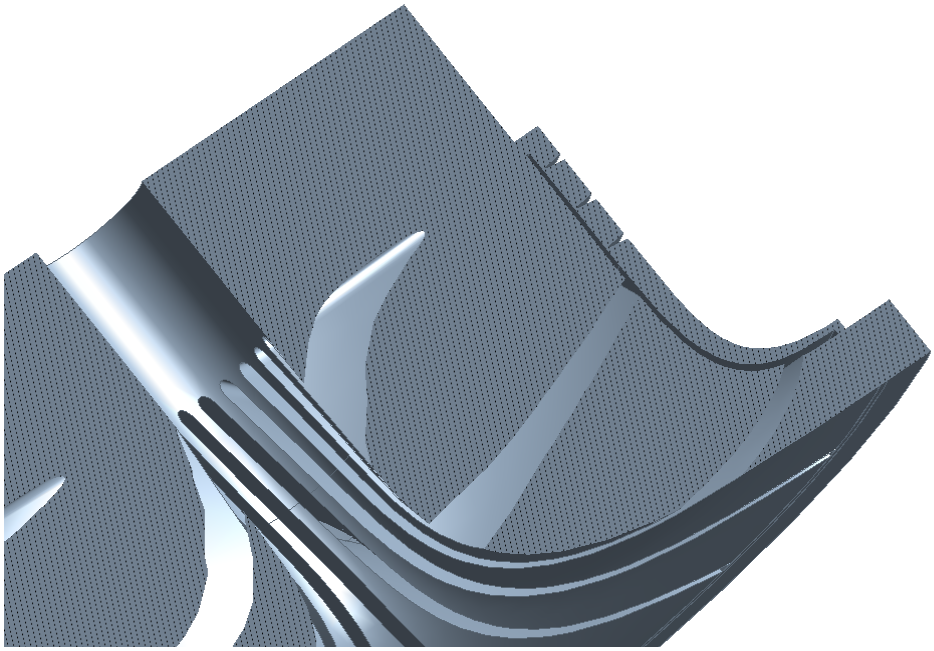

Figure 4: A cross section of the computational fluid domain of the compressor system from Song et al.

Results

To calculate the flow coefficient from the results of the CFD analysis, a similar equation was used that is described in the experiment by Song et al. [Song et al., 2019]. The rotor radius was added to the bottom of the equation to account for the surface speed.

$$\Phi = \frac{m_i}{\rho_i \omega D^3} \tag{2}$$

The above equation is used to calculate the flow coefficient of the impeller, shroud, and seal system. The density used was 1.16 kg/m^3. This value was not given in the experimental paper by Song et al., but it is the value of the density of air at the given inlet temperature. The rotating speed in the equation was converted to rad/s, yielding a value of 3862.2 rad/s.

Using this equation, the calculated flow coefficient from the model calculated mass flow of 0.0656 gave a flow coefficient of 0.0651. The flow coefficient in the experiments by Song et al. was 0.063, meaning there was only a 3.33% error between the results.

Conclusion

Using CFD analysis, the flow coefficient from the experimental paper was successfully validated against the results from the virtual model. This result verifies that the CFD simulation of the shrouded impeller model gave accurate results with regards to leakage and the flow coefficient of the design.

More work is required to verify the rotordynamic coefficients of the ANSYS model against the experimental results from the original paper. Mesh convergence became an issue

when simulated the CFD model to determine the forces on the impeller. These issues prevented calculation of the rotordynamic coefficients, which would have been validated against the experimental numbers. Future research can build upon the existing model and mesh in order to calculate the rotordynamic coefficients using ANSYS.

CFD ANALYSIS OF SHROUD SURFACE TEXTURING ON THE EFFICIENCY AND STABILITY OF A SHROUDED CENTRIFUGAL COMPRESSOR

Introduction

Rotordynamic forces arise when a working fluid in turbomachinery interacts with a moving rotor and acts on it in various directions. These forces cause instability which can eventually lead to mechanical failure of the machinery. This makes reduction of these forces, and the ability to predict what model will best do this, essential to the design of turbomachinery.

The potential benefits of various types of seals have already been heavily analyzed, both experimentally and computationally. Labyrinth seals are well known to control leakage with minimum rise in temperature and torque. These seals are commonly used in the construction of turbomachinery because of these benefits, as well as the wide range of speeds and pressures they can be operated at [Chupp et al.].

Simulations have been run on modeled labyrinth seals to determine the effect of changing various parameters on compressor performance. Tang et al. used CFD analysis to modify the tooth angle, clearance, and cavity depth [Tang et al., 2017].

Other types of seals have also been investigated to determine the effects of their implementation on the performance of centrifugal compressors. Spiral grooves were analyzed in their used with dry gas compressors by Shah. This study concluded that spiral grooved seals provide force balancing and stability to dry gas compressors [Shah].

CFD analysis on leakage flows in the shroud cavity of a centrifugal compressor have been studied historically by Soldatova. These results, however, only looked at shroud cavities with smooth surfaces and no texture [Soldatova, 2017].

A full system of impeller, shroud, and seal has been simulated using CFD analysis historically, however this model also had no surface texturing and didn't examine how such a change could affect the leakage flow in the compressor. [Song et al.]

Historically, no testing on the surface texturing of an impeller shroud cavity has been conducted. This paper uses CFD analysis to determine the effect from various types of surface textures on compressor performance. With CFD simulation, many textures can be easily modeled and tested without the high costs of experimental testing.

The full impeller, shroud, and seal system from Song et al. was modeled in addition to the shroud cavity model from Soldatova's study, and the same surface textures were applied to each geometry so the results could be compared. While the models created in Soldatova and Song et al. were similar in that they both had labyrinth seals, the shroud cavity width was more standard in Soldatova's model and smaller than usual in the model from Song et al.. By performing CFD analysis on both of these models, the effect of surface texturing on leakage flow in centrifugal compressors could be examined for both a normally sized shroud cavity and a smaller than normal one.

1. Geometries

Multiple geometries were designed with the intent of diminishing leakage flow and improving the stability of the compressor. Both the interior surfaces of the shroud cavity up to the seal teeth and were textured to best improve performance and have the greatest effect on reducing leakage.

The base for half of the geometries is the same impeller-shroud-seal system used in the experimental paper by Song et al. [Song et al., 2019].

Table 4. Geometric Parameters for Song et al.

Parameter	Value
Impeller exit diameter (D)	153.24 mm
Blade exit length (d)	9.19 mm
Back-sweep angle	44.5 degrees
Number of blades	16
Number of seal teeth	3
Seal clearance (C)	0.55 mm
Seal height (h)	3 mm
Seal pitch (L)	7 mm
Rotor radius (R)	46.79 mm
Shroud cavity height at inlet (1)	1.38 mm
Shroud cavity height at middle (2)	2.5 mm
Shroud cavity height at exit (3)	3.55 mm

The clearances are kept the same for each of the new designs. This ensures a clear comparison can be drawn between each of the surface textured systems and the original system.

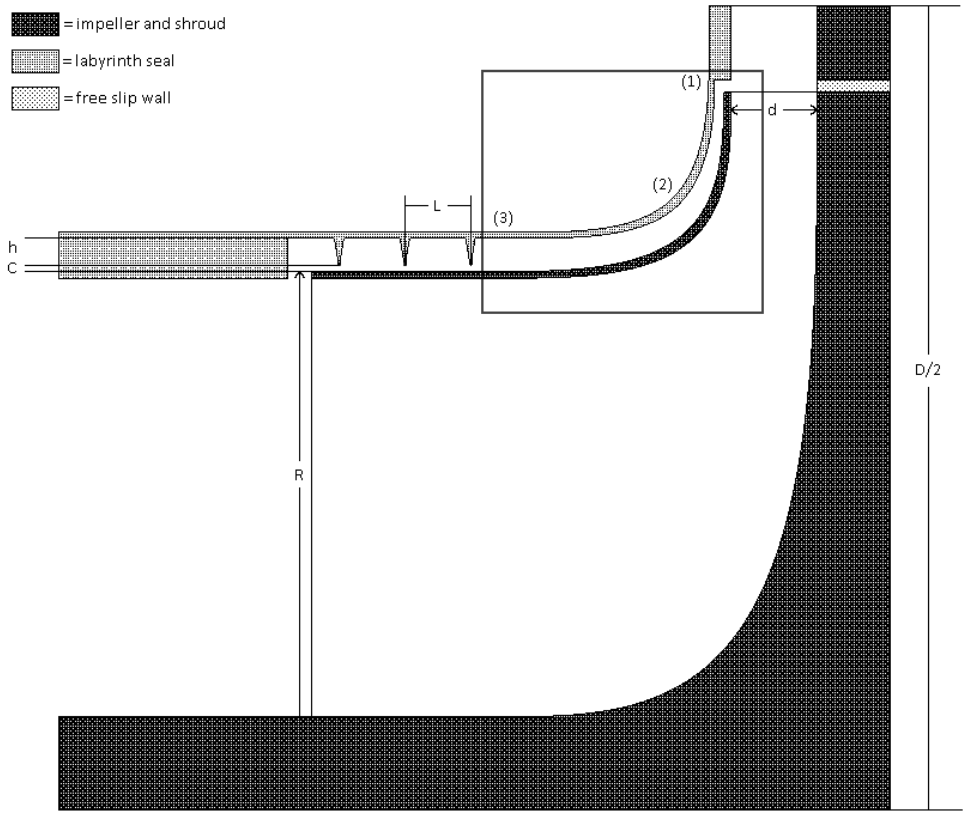

Figure 5: The original, untextured geometry from Song et al.

The textures of the surfaces of the shroud and the seal were both altered to most change the flow pattern inside the cavity. The rectangular box over the shroud cavity in Figure 5 shows where the following figures of the various textures are located on the seal and shroud system.

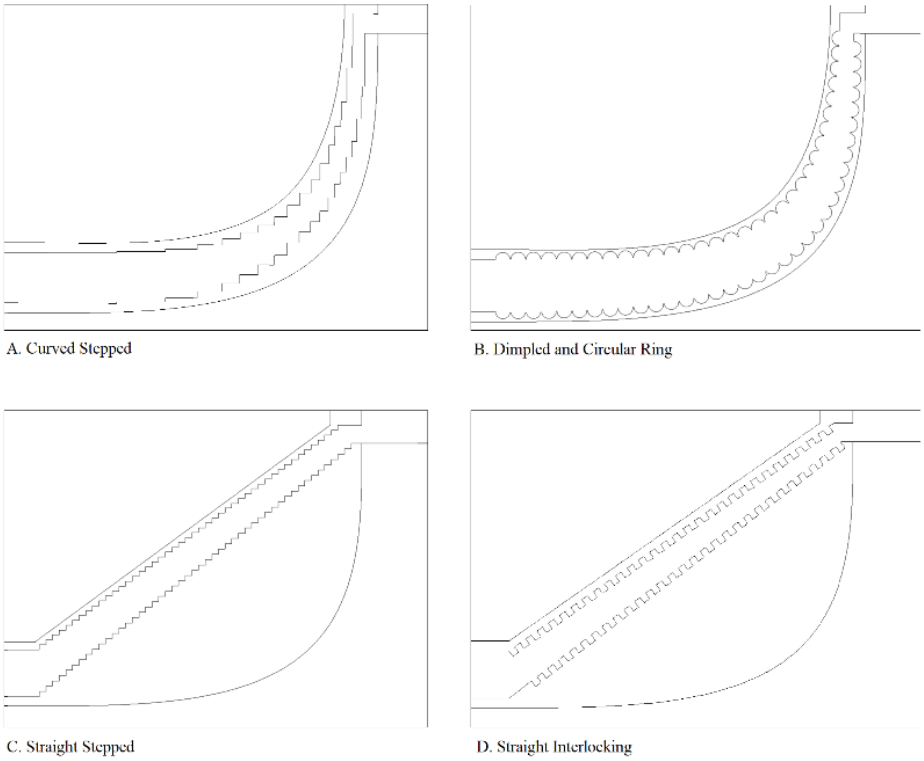

Figure 6: Cross sections of the textured designs on the Song et al. model.

The shroud cavity modeled and tested by Soldatova was also created for this study, with each of the same textures modeled with the Song impeller. This model had a more typical shroud gap width than the Song design, so was used to validate that the surface texturing in a shroud cavity would still have an effect even with a larger clearance. The geometric parameters for this shroud cavity design are listed in Table 5 below.

Table 5. Geometric Parameters for Soldatova

Parameter	Value
Impeller exit diameter (D_2)	409.85 mm
Number of seal teeth	4
Seal clearance (C_2)	0.50 mm
Rotor diameter (D_R)	204.95 mm
Shroud cavity height at inlet (b_2)	5.94 mm

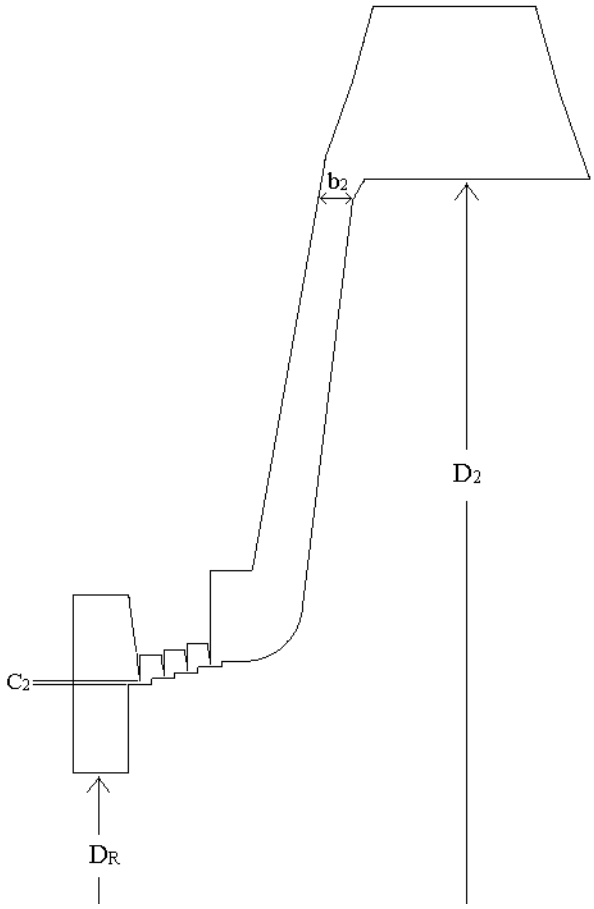

Figure 7: The untextured shroud cavity Soldatova model cross section.

The textures created on the Soldatova shroud cavity model were the same ones created for the Song et al. model, just scaled according to the different impeller exit diameters from the two models. The ratio between D_2 and D is 2.67. This value was then multiplied by the values used in Song et al.'s textured models to get the correct dimensions that were used for the Soldatova textured models.

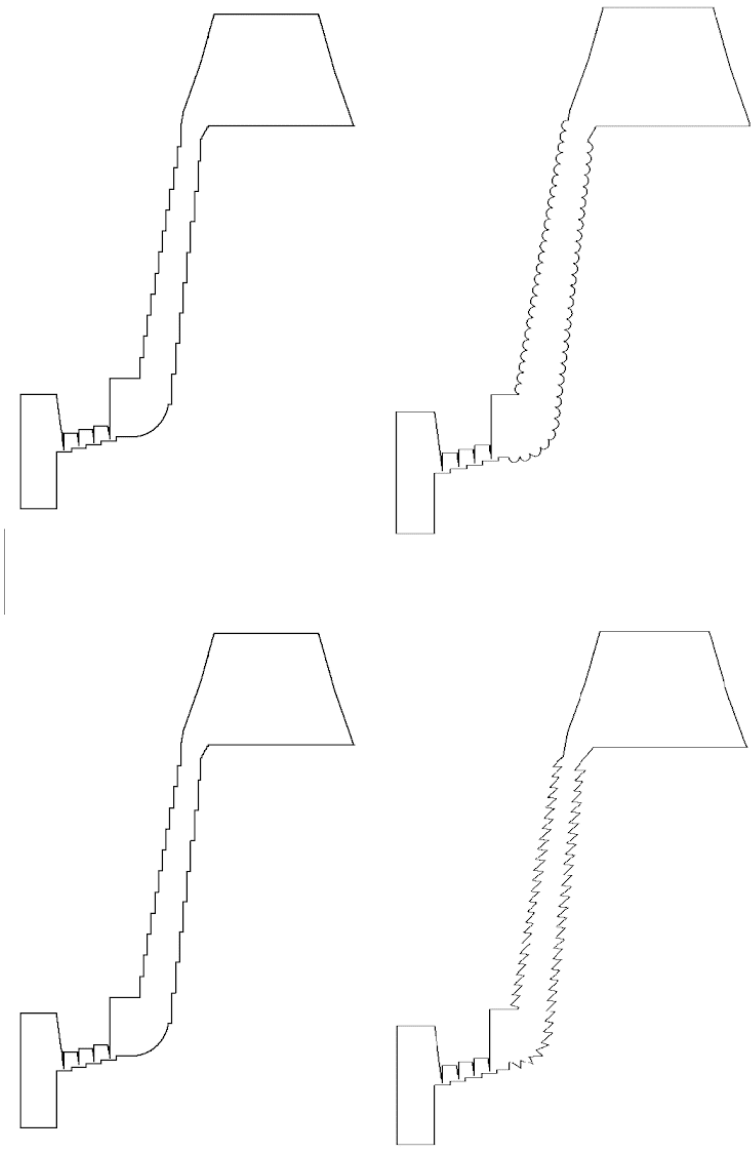

Figure 8: Cross sections of the textured designs on the Soldatova model.

Future Work

Due to time constraints, the ANSYS model could not be correctly meshed in the software, a step required to simulate the running of the impeller system in order to find the rotordynamic coefficients. Future research can build upon the existing models of various surface textures in order to calculate the rotordynamic coefficients and forces acting on each system. Through this work, the best surface texture for reducing aerodynamic cross coupling can be identified.

CFD VALIDATION OF ROTORDYNAMIC FORCES IN A LIQUID SMOOTH ANNULAR SEAL

Introduction

Annular seals that are fed with an incompressible liquid are common in high speed rotating machinery. The effects of these types of seals are noticeable on the performance of the machinery as a whole [Jolly et al., 2018]. If the rotordynamic coefficients can be determined through a computer simulation of machinery before that machinery is used in a physical space, money can be saved through reducing repairs or maintenance required, and the efficiency of the machine can be improved.

Smooth, annular seals are used as components in turbomachinery for various purposes. Seals fed with a liquid working fluid can reduce leakage between areas of different pressures within turbomachinery. Annular seals specifically have a clearance between the rotor and stator, allowing for non-contacting rotation in operation. These types of smooth seals can serve to enhance rotordynamic stability and reduce vibrational effects during machinery operation [Darden et al., 1999]. Eccentricity of the rotor within the stator can generate a shaft reaction force as opposing regions of high and low fluid pressure are created [Ahmed et al., 2018].

A constant no matter the purpose of the seal is that they always rely on stability and low vibration levels to operate efficiently and safely. Typically, the higher the speed of the rotor, and the smaller the clearance in the seal, the more benefit can be achieved from the seal. On the other hand, making these changes to a seal also tends to lead to more unstable and unpredictable motion. Smooth seals are known to suffer from more leakage, but have better rotordynamic stability than other types of seals, such as a grooved seal where there is texture on the stator component. This unstable movement is also exacerbated if there is even a slight offset of the rotor within the stator [Torres, 2016].

This destabilizing effect can be observed in operating machinery over time. To better understand the effects of whirl on a smooth seal, this type of turbomachinery has previously been physically modeled. The stiffness and damping coefficients can be determined from an experimental simulation, and these indicate the potential for instability in the seal. The benefit of doing this type of testing experimentally first, is that a computer model can then be made with the same parameters in order to verify the CFD results. Experimental tests have been conducted on a long smooth seal with a mixed fluid flow. Silicone oil and air were combined to test the effects of mixed-flow on the stability of a smooth seal. The gas-volume fraction (GVF) is varied from 0-10% so that the fluid is primarily liquid, and no eccentricity is introduced. This research found that there were reduced direct stiffness coefficient results, and that CFD analysis can be used in future to compare results [Tran et al., 2020].

CFD analysis has previously been used to analyze annular seals in pumps to determine leakage and rotordynamic characteristics. This existing research studied a seal fed with water as the working fluid and with a range of eccentricities. This research verified that 3D CFD analysis provides accurate results for leakage prediction. The study confirmed that there was room for improvement regarding prediction of the rotordynamic coefficients of an annular seal modeled with CFD [Ha, 2012]. A study was also conducted by Wu et al. on a transient method using 3D CFD analysis. This research confirmed that the transient method gave accurate results, like a traditional 3D CFD analysis on a liquid smooth annular seal, but with less computational time. The results of this research were validated against the experimental results of a smooth annular seal [Wu et al., 2016].

The goal of this research is to use CFD analysis to determine the rotordynamic coefficients of a smooth seal fed with water as the eccentricity varies. This computer model is built based on an experimental one previously tested by Jolly et al.. This research would be beneficial in testing other smooth seals with different boundary conditions or geometry without the need to build a costly physical testing rig to run experiments on.

Procedure

1. **Geometry**

The smooth seal modeled in this study is taken from the experimental study conducted by Jolly et al. on both smooth and round-hole pattern water fed annular seals [Jolly et al., 2018]. In this physical study, hot water is used as the working fluid and runs through rotating seals that are both smooth and textured. For the CFD replication of this experiment, only the smooth seal was modeled and used. The rotor is offset at a range of ratios inside the stator, from 0.1 to 0.7 of the clearance. The geometry modeled is the fluid domain of the smooth seal used by Jolly et al.

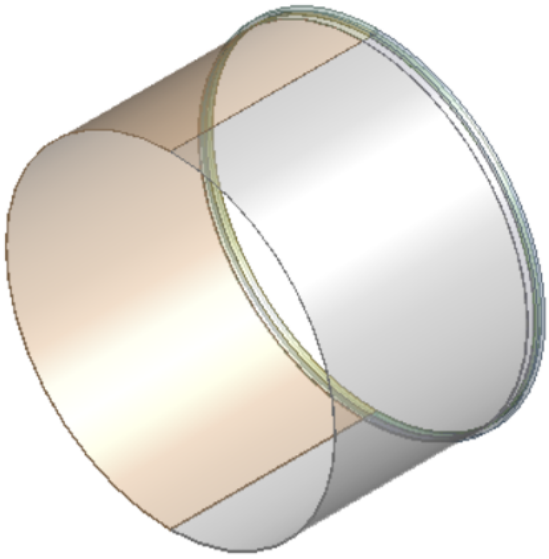

Figure 9: Model of the smooth seal in ANSYS-CFX.

A region is added to the inlet that has a greater radius than the main fluid region of the seal. This is done so that the entrance loss effects are captured as fluid flows in through the boundary. This same region is not required at the outlet, and the outlet region is seen as smooth in Figure 1 above.

Table 6. Geometric Parameters

Parameter	Value
Seal Diameter (D)	240 mm
Seal Length (L)	150 mm
Seal Clearance (C)	0.57 mm
Inlet Height (h)	5 mm

The values given for the experimental model used by Jolly et al. are simply L/D = 0.625 and C/R = 0.00475. The values used in the CFD model were then chosen based on these parameters to ensure the ratios matched. The height of the inlet for entrance loss effects was chosen to be much larger than the clearance so that it is adequate.

2. Numerical Methodology

The computational model of the smooth seal was designed in ANSYS-CFX using the geometric parameters given in Table 1. Because of the simple model design, the mesh was easy to generate and no features had to be oversimplified to fit with elements. The mesh was generated using an element size of 0.57 mm to match the size of the clearance. The number of elements was 7,590,840 and the mesh type was one with rectangular elements.

To account for the movement of the fluid around the inlet region, inflation layers were added by the inlet. Slices were also added to the geometry, one that ran the entire length of the seal and another that was 5 mm into the clearance region and was circumferential. These aided in sweeping the mesh as well as generating the inflation layers while keeping rectangular elements. To ensure that the entire model allowed fluid flow smoothly through all the sections, the geometry was made into 1 part after the slices were added.

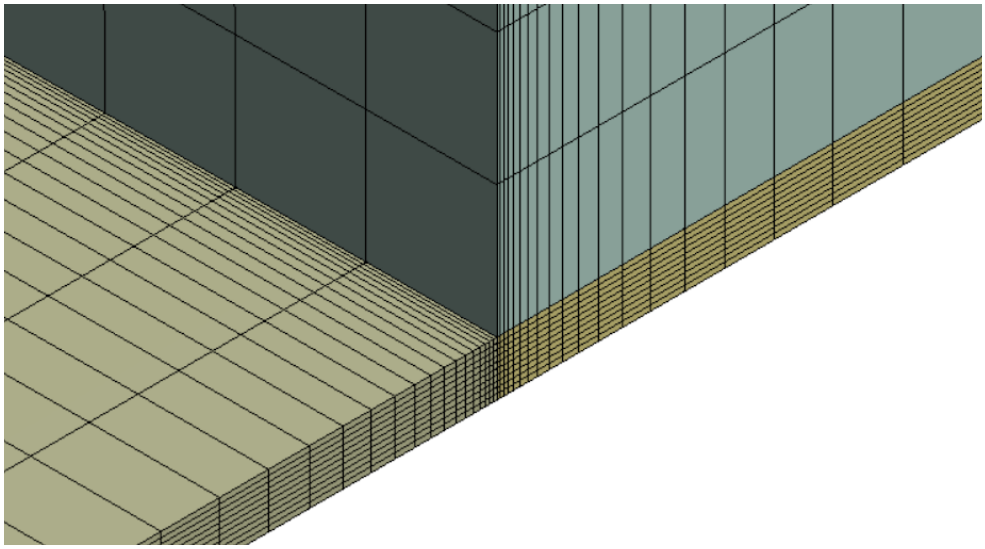

Figure 10: The inflation layers of the mesh on the inlet region of the model.

Two rotating speeds were used, to match the rotating speeds used in the experimental paper that the model is based on. The inlet and outlet boundary conditions were also set to match those from the paper.

Table 7. Boundary conditions from Jolly et al.

Parameter	Value
Fluid	Water
Temperature	40 °C
Preswirl	0
Inlet Pressure	5 bar (Opening Pres. and Dirn)

Outlet Pressure	0 bar (Opening Pres. and Dirn)
Rotating speed	50, 6000 RPM

The inlet and outlet boundaries were set as opening boundaries in the Setup section of ANSYS-CFX. This condition allows fluid to flow in either direction through these sections of the geometry. Due to the pressure difference also set at these boundaries, shown in Table 7 above, fluid only flowed through the model in the direction of inlet to outlet, moving from higher to lower pressure. The values for pressure at the openings were taken from the experimental model used by Jolly et al., where the values used were 10 bar from the inlet and 5 bar for the outlet.

The inside surface of the fluid region was set to the two rotating speeds for the various tests, as this was the section of the geometry against the rotor, and the outside surface was set to stationary. The establishment of the 8 pieces of the model as 1 part in the Geometry creation meant that fluid flowed freely between them without the need for additional boundary conditions connecting the surfaces.

With the mesh generated, the model could be tested at the eccentricities of the varying ratios of the clearance. This range of eccentricities allowed the force results to be compared based on how eccentric the rotor was during operation. Equations were used with the values of the X and Y forces on the rotor as well as the eccentricity to calculate the 4 rotordynamic coefficients in the seal.

Results

Using the X and Y forces on the rotor to calculate the rotordynamic coefficients in the model required equations that also used the eccentricity at that point. The offset of the rotor within the stator to create the eccentricity was in the Y direction, resulting in the following equations:

$$K_{xy} = \frac{-F_x}{e}$$
$$K_{xx} = \frac{-F_y}{e}$$
$$C_{xx} = \frac{1}{628.3}\left(K_{xy} - \frac{F_x}{e}\right)$$
$$C_{xy} = \frac{1}{628.3}\left(-K_{xx} + \frac{F_y}{e}\right) \quad (3)$$

Where K_{xy} is the cross-coupled stiffness, K_{xx} is the direct stiffness, C_{xx} is the direct damping, and C_{xy} is the cross-coupled damping. The forces on the rotor F_x and F_y were provided by the software in Newtons (N) and e is the eccentricity in meters (m). These coefficients could be used to determine how much the eccentricity of the rotor within the stator affected the stability and efficiency of the entire seal part.

To initially validate the model, the results for the 0.1 eccentricity ratio are compared. These results show good agreement between the calculated coefficients at 50 and 6000 rpm. After this validation is confirmed, the results of the simulated model at various frequencies can be treated as accurate.

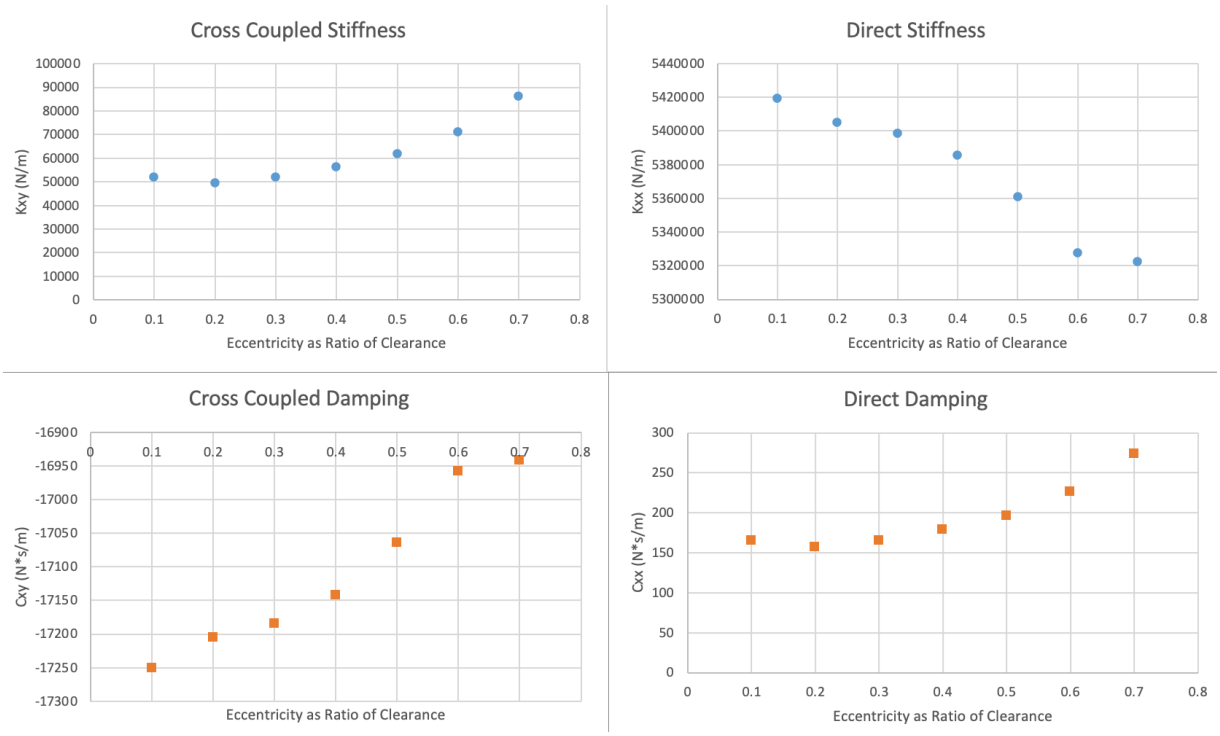

Figure 11: Graphs showing calculated rotordynamic coefficients vs. the eccentricity ratio.

In order to better analyze the stability of the smooth seal in relation to the eccentricity ratio, effective damping can be calculated from the rotordynamic coefficients using the following equation:

$$effective\ damping = K_{xy} - (\omega * C_{xx}) \tag{4}$$

Conclusion

From the data, effective damping was found to decrease as eccentricity increased. This trend suggests that stability of the smooth seal system may be overestimated by bulk flow prediction when the eccentricity ratio is large due to bulk flow predictions being based on the assumption of small eccentricity.

Future work can further validate these results with more cases and using more experimental data of similar smooth seal systems.

CFD VALIDATION OF ROTORDYNAMIC FORCES IN A GAS SMOOTH ANNULAR SEAL

Introduction

Annular seals in turbomachinery are used to reduce vibrational effects on machinery performance. These types of seals, whether fed with a liquid or a gas, enhance stability and lower vibration response during machine operation [Darden et al., 1999]. The geometry of smooth annular seals involves a floating rotor surrounded by a clearance region and a stator that self-centers during operation. Common uses for annular seals in turbomachinery include steam turbines

and high-pressure compressors. In these applications, smooth seals address leakage and stability issues [Kerr, 2004].

Smooth gas seals are used in turbomachinery limit leakage between different regions of the machinery that are at different pressures. To improve the performance of machinery, these seals are operated at higher rotating speeds with smaller clearances . Any slight eccentricity of offset in the rotor within the stator exacerbates unstable movement of the machinery during operation [Childs et al., 1995].

CFD analysis has been performed on annular plain gas seals by Ha et al. in order to predict rotordynamic coefficients and leakage. Using Fluent Ver 6.3 software, that existing research confirmed that 3D CFD analysis was appropriate for predicting characteristics of annular gas seals where air is used as the fluid [Ha, 2014]. This existing research confirms that CFD analysis is appropriate for studying annular gas seals, but does not use CFD software to examine how eccentricity affects the rotordynamic characteristics of the seal.

Smooth seals have additionally been modeled and tested using CFD analysis in wet gas conditions. These conditions are where small liquid particles are dispersed in the gas. The study conducted by Li et al. used air as the working fluid with Silicone oil particles interspersed in the gas. The CFD modelling of the seal proved to be accurate when compared to experimental results. This study showed that the liquid volume fraction (LVF) of liquid in the gas had a significant effect on both leakage and rotordynamic coefficients of the smooth gas seal [Li et al., 2019]. Zhang et al. additionally studied a long smooth seal with two phase, mainly-air fluid mixtures. The experimental study showed that decreased clearance significantly reduced the leakage rate, and that the cross-coupled stiffness (k) and direct damping coefficient (C) decrease as the clearance increases with a purely air fluid. There was no eccentricity introduced in this study of a smooth gas seal [Zhang et al., 2019].

There exists an experimental study from Childs et al. that has examined how eccentricity generates destabilizing rotordynamic forces in smooth gas seals. This experimental study was performed using a physical rig, and confirmed that stability of an annular gas seal has a strong dependence on the eccentricity of the rotor within the stator. This research looks to confirm that a computational model can be generated and accurately simulate the effects of eccentricity on seal stability. Using the same geometry and boundary conditions, a computer model can be created and the results of CFD analysis used. If this computational study proves to be accurate when compared to the results of the physical experiment, CFD analysis can, in future, be used with different geometries of smooth gas seals to determine how large the rotordynamic coefficients will be for various eccentricities. CFD analysis requires a computer but not the use of an expensive, physical rig. This knowledge would be beneficial in reducing the cost of testing potential smooth annular gas seals when designing turbomachinery.

Procedure

1. Geometry

The geometry for the model used in ANSYS-CFX was created using the same dimensions as the physical seal used in the experiment from Childs et al.. The fluid domain through which the gas flows is what is modeled computationally. An extra region is added at the inlet, large enough to account for any entrance loss effects as the fluid enters the seal clearance region. The eccentricity of the rotor within the stator was also varied throughout the tests, along a range of ratios of the clearance. These values matched those experimentally tested by Childs et al. so that

the computational results could be compared for accuracy. The dimensions of this experimental model are given in the table below.

Table 8. Geometric Parameters

Parameter	Value
Seal Diameter (D)	152 mm
Seal Length (L)	50.8 mm
Seal Clearance (C)	0.41 mm
Inlet Height (h)	5 mm
Eccentricity ratio	0 - 0.5

To successfully generate a mesh in the next steps of model generation, the geometry had to be divided into 8 pieces, and then combined into 1 part. This allowed the program to recognize the full geometry as one fluid region, while giving clearer boundaries on where to start the various meshing methods required for the model.

2. Numerical Methodology

To simulate the model computationally, a mesh had to be generated on the geometry. The function was chosen to generate the mesh in ANSYS-CFX. This mesh had rectangular elements to fit the smooth seal geometry. The maximum size of the elements was set to match the clearance of the model (0.41 mm). Inflation layers were added to the mesh to account for fluid movement between the inlet and clearance region. These inflation layers were generated using the first layer thickness method in ANSYS-CFX. The number of elements in the mesh was 2,011,392 and the mesh type was one with rectangular type elements.

Generating the mesh with rectangular elements across the entire geometry required that the model be split into 8 sections combined into one part in the software. This technique allowed the elements to generate uniformly across the entire inlet and clearance regions. The slices in the model also allowed the sweep methods used for the mesh to generate from distinct faces within the geometry. Both circumferential and radial sweep methods were used when creating the mesh. Circumferential sweeps were applied to the 6 clearance region pieces, sweeping from the inside surface against the rotor to the outside surface that borders the stator. A radial sweep was used for the larger 2 inlet regions.

The boundary conditions set for the model matched those given by the experimental paper from Childs et al.. The fluid used in the smooth gas seal was air at nearly room temperature. Two rotating speeds were used in the experimental paper, so two are used in this CFD analysis to confirm the results are accurate at various speeds.

Table 9. Boundary conditions

Parameter	Value
Fluid	Air
Temperature	300.7 K
Preswirl	0

Inlet Pressure	7.918 bar (Opening Pres. and Dirn)
Outlet Pressure	5.441 bar (Opening Pres. and Dirn)
Rotating speed	5000, 16000 rpm

The inlet and outlet boundaries were set as opening boundaries in the Setup section of ANSYS-CFX. This meant that fluid could flow in either direction through these sections of the geometry. Due to the pressure difference also set at these boundaries, fluid only flowed through the model in the direction of inlet to outlet, moving from higher to lower pressure. The inside surface of the fluid region was set to the two rotating speeds, as this was the section of the geometry against the rotor, and the outside surface was set to stationary.

Using the two rotational speeds and the range of eccentricities, simulations were run to determine the rotordynamic coefficients at each set of parameters. In order to calculate the values of the rotordynamic coefficients, the forces on the rotor in the X and Y directions were used. These force values in Newtons could easily be obtained from the results tab in ANSYS-CFX.

Results

The results obtained from the simulation in ANSYS-CFX were the values of force in Newtons on the rotor in the X and Y directions. These values can then be converted into rotordynamic coefficients, the type of value required to compare the results to the experimental paper, using the 4 equations given previously as equation set 3 for the Jolly et al. smooth seal model.

K_{xy} is the cross-coupled stiffness, K_{xx} is the direct stiffness, C_{xx} is the direct damping, and C_{xy} is the cross-coupled damping. The forces on the rotor F_x and F_y were provided by the software in Newtons (N) and e is the eccentricity in meters (m). Once these coefficients were calculated, they could be compared against the coefficients in the experimental paper to validate the computational results.

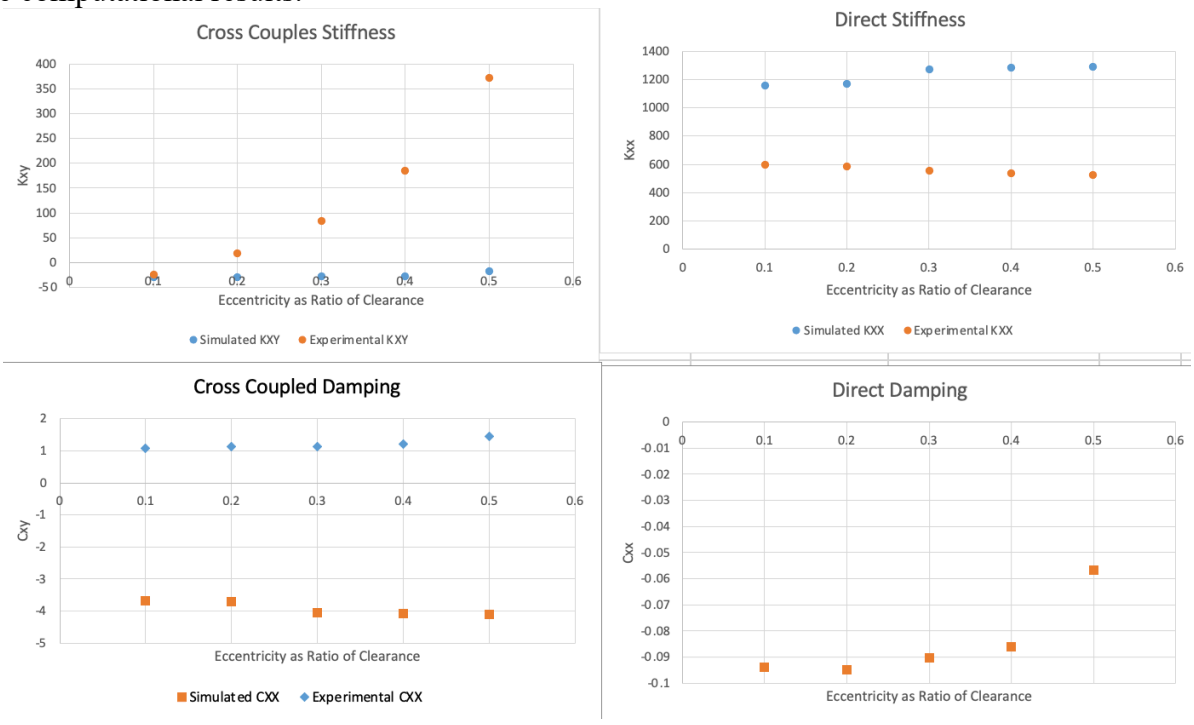

Figure 12: Graphs showing calculated rotordynamic coefficients vs. the eccentricity ratio for the Childs et al model.

Conclusion

The calculated results from the CFD model created in ANSYS are slightly off from the expected results based on the experimental paper. The results found through this research show trends that are correctly produced by the simulation, but further improvements are required to attain results closer to the experiment.

Future work can focus on improving the CFD model and geometry to better match the Childs et al. smooth gas seal. This work could generate results that then better match the experimental data and validate the ANSYS simulation. This would be useful in testing the geometry of any other smooth gas seals for rotordynamic forces and stability.

REFERENCES

Ahmed Bin Najeeb, Ovais; Childs, Dara (2018). Static and Rotordynamic Analysis of a Plain Annular (Liquid) Seal in the Laminar Regime with a Swirl Brake for Three Clearances. Turbomachinery Laboratory, Texas A&M Engineering Experiment Station. Available electronically from http : / /hdl .handle .net /1969 .1 /172501.

Childs, D. W., 1989, "Fluid-Structure Interaction Forces at Pump-Impeller-Shroud Surfaces for Rotordynamic Calculations," Journal of Vibration, Acoustics, Stress, and Reliability in Design, 111(3), pp. 216-225.

Childs, D. W., Alexander, C. R., and Yang, Z. (January 1, 1995). "Theory Versus Experiment for the Rotordynamic Characteristics of a Smooth Annular Gas Seal at Eccentric Positions." ASME. *J. Tribol*. January 1995; 117(1): 148–152. https://doi.org/10.1115/1.2830591

Chupp, Raymond E., Robert C. Hendricks, Scott B. Lattime, and Bruce M. Steinetz. "Sealing in Turbomachinery." *Journal of Propulsion and Power* 22, no. 2, 313-49. Aerospace Research Central.

Darden , J. M., Earhart, E. M., and Flowers, G. T. (March 1, 1999). "Comparison of the Dynamic Characteristics of Smooth Annular Seals and Damping Seals ." ASME. *J. Eng. Gas Turbines Power*. October 2001; 123(4): 857–863. https://doi.org/10.1115/1.1383256

Guinzburg, A., C. E. Brennen, A. J. Acosta, and T. K. Caughey. "Experimental Results for the Rotordynamic Characteristics of Leakage Flows in Centrifugal Pumps." *Journal of Fluids Engineering* 116, no. 1 (1994). doi:10.1115/1.2910217.

H N Tang et al 2017 IOP Conf. Ser.: Mater. Sci. Eng. 164 012015

Ha, T.W., Choe, B.S. Numerical prediction of rotordynamic coefficients for an annular-type plain-gas seal using 3D CFD analysis. *J Mech Sci Technol* 28, 505–511 (2014). https://doi-org.proxy01.its.virginia.edu/10.1007/s12206-011-0830-3

Ha, T.W., Choe, B.S. Numerical simulation of rotordynamic coefficients for eccentric annular-type-plain-pump seal using CFD analysis. *J Mech Sci Technol* 26, 1043–1048 (2012). https://doi.org/10.1007/s12206-012-0217-x

Iwatsubo, T., 1980, "Evaluation of Instability Forces of Labyrinth Seals in turbines or Compressor " Proc. NASA t Conference Publication 2133: Rotordynamic Instability Problems in High-Performance Turbomachinery - 1980, pp. 139- 167.

Jolly, P., Arghir, M., Bonneau, O., and Hassini, M. (July 5, 2018). "Experimental and Theoretical Rotordynamic Coefficients of Smooth and Round-Hole Pattern Water-Fed Annular Seals." ASME. *J. Eng. Gas Turbines Power*. November 2018; 140(11): 112501. https://doi.org/10.1115/1.4040177

Kamouni, Mohamed. "CFD Predictions of Induced Fluid Forces and Dynamic Coefficients for a Compressor Eye Seal." *International Journal of Scientific & Engineering Research* 7, no. 9 (September 2016): 429-36.

Kerr, Bradley Gray (2004). Experimental and theoretical rotordynamic coefficients and leakage of straight smooth annular gas seals. Master's thesis, Texas A&M University. Texas A&M University. Available
electronically from http : / /hdl .handle .net /1969 .1 /1518.

Kim, Eunseok. "CFD Based Prediction of Rotordynamic Coefficients and Stability Analysis for Centrifugal Pump/Compressor." PhD diss., Texas A&M University, 2016.

Li, Z., Fang, Z., and Li, J. (October 4, 2018). "Numerical Investigation on the Leakage and

Rotordynamic Characteristics for Three Types of Annular Gas Seals in Wet Gas Conditions." ASME. *J. Eng. Gas Turbines Power*. March 2019; 141(3): 032504. https://doi.org/10.1115/1.4041313

Muttalli, Raghavendra S., Shweta Agrawal, and Harshla Warudkar. "CFD Simulation of Centrifugal Pump Impeller Using ANSYS-CFX." *International Journal of Innovative Research in Science, Engineering and Technology*03, no. 08 (2014): 15553-5561. doi:10.15680/ijirset.2014.0308066.

Shah, Piyush. "Dry Gas Compressor Seals." Proceedings of The Seventeeth Turbomachinery Symposium.

Soldatova, K. (2017). CFD study of leakage flows in shroud cavities of a compressor impeller. *IOP Conference Series: Materials Science and Engineering, 232,* 012045. Doi: 10.1088/1757-899x/232/1/012045

Song, Jieun, Suyong Kim, Tae Choon Park, Bong-Jun Cha, Dong Hun Lim, Joo Sung Hong, Tae Wook Lee, and Seung Jin Song. "Non-Axisymmetric Flows and Rotordynamic Forces in an Eccentric Shrouded Centrifugal Compressor." Proceedings of ASME Turbo Expo 2019: Turbomachinery Technical Conference and Exposition, Arizona, USA, Phoenix.

Torres, Jose Maria (2016). Static and Rotordynamic Characteristics of Liquid Annular Seals with a Circumferentially-Grooved Stator and Smooth Rotor using Three Levels of Circumferential Inlet-Fluid Rotation. Master's thesis, Texas A & M University. Available electronically from http : / /hdl .handle .net /1969 .1 /174638.

Tran, D. L., Childs, D. W., Shrestha, H., and Zhang, M. (January 29, 2020). "Preswirl and Mixed-Flow (Mainly Liquid) Effects on Rotordynamic Performance of a Long ($L/D = 0.75$) Smooth Seal." ASME. *J. Eng. Gas Turbines Power*. March 2020; 142(3): 031012. https://doi-org.proxy01.its.virginia.edu/10.1115/1.4044291

Wu, D., Jiang, X., Li, S. *et al.* A new transient CFD method for determining the dynamic coefficients of liquid annular seals. *J Mech Sci Technol* 30, 3477–3486 (2016). https://doi-org.proxy01.its.virginia.edu/10.1007/s12206-016-0707-3

Zhang, M., Childs, D. W., Tran, D. L., and Shrestha, H. (October 29, 2018). "Clearance Effects on Rotordynamic Performance of a Long Smooth Seal With Two-Phase, Mainly-Air Mixtures." ASME. *J Eng Gas Turbines Power*. January 2019; 141(1): 012502. https://doi.org/10.1115/1.4040809